Rare earth chemistry of perovskite group minerals from the Gardiner Complex, East Greenland

LINDA S. CAMPBELL*, PAUL HENDERSON, FRANCES WALL

The Natural History Museum, Cromwell Road, London SW7 5BD, UK

AND

TROELS F. D. NIELSEN

Øster Voldgade 10, 1350 Copenhagen K, Denmark

Abstract

Perovskite group minerals, general formula ABX_3, from the intrusive ultramafic alkaline Gardiner Complex, East Greenland, range from almost pure $CaTiO_3$ (perovskite, *sensu stricto*), to the rare earth element (*REE*) variety, loparite-(Ce). Chemical zonation in the perovskites (*sensu lato*), is described by the substitutions $2Ca^{2+} = (Na^{+} + REE^{3+})$ on the *A*-site and $2Ti^{4+} = (Fe^{3+} + Nb^{5+})$ on the *B*-site. Other trace elements detected include Th, Sr, Al, Si, Zr, Ta and Sn. Excellent agreement was found between the determinations of the *REE* by electron microprobe and neutron activation analysis. Chondrite-normalized *REE* patterns display enrichment in the light rare earths for perovskite, loparite, apatite, melilite and diopside. Mean perovskite/apatite partition coefficients from four of the Gardiner rocks were calculated as La = 10.4, Ce = 13.8, Nd = 13.9, Sm = 9.9, Eu = 7.7, Gd = 5.2, Tb = 5.6, Tm = 5.5, Yb = 2.7 and Lu = 1.6, indicating that perovskite concentrates all *REE* to a much greater extent than apatite. Light-*REE* enrichment occurs in both perovskite and apatite.

KEYWORDS: rare earth elements, perovskite, apatite, loparite, Gardiner Complex, Greenland.

Introduction

THE Gardiner Complex, East Greenland is an alkaline igneous intrusion of Tertiary age consisting of an ultramafic suite and a later ring-dyke system of melilitolites, syenites and carbonatites. It has been described by Frisch and Keusen, (1977), Nielsen, (1979, 1980, 1981, 1994), Johnsen *et al.* (1985), Nielsen and Holm, (1993) and Nielsen *et al.* (in press). The age of the magmatic activity, by a fission track method, is 50 Ma (Gleadow and Brooks, 1979). Perovskite occurs in the dunites of the ultramafic suite, the later magmatic melilitolites and associated rocks. In these later rocks, it may attain significant modal percentages (up to about 20%), while occasionally very high abundances occur, resulting in perovskitite. A brief description of the occurrence of perovskite in the Gardiner Complex is given by Frisch and Keusen (1977) who also provided an analysis of perovskite from a melanite–perovskite rock together with a microprobe profile of a zoned grain. Their data show that this perovskite is calcium titanate with minor substitution of Na, Nb and the light rare earth elements (*REE*) at about 7 wt.% REE_2O_3.

Models for the classification of perovskite group minerals have been provided by Nickel and McAdam (1963) and Mitchell (1996) but there is still much to be learned about their chemical systematics with respect to both major and trace element substitutions. The rocks of the Gardiner intrusion offer an ideal starting point for a study of the mineral chemistry of perovskite because the perovskite is relatively abundant, there is some variation in composition from pure $CaTiO_3$ towards loparite, it occurs in association with other well-characterised minerals

* Present address: School of Geological Sciences, Kingston University, Penrhyn Road, Kingston upon Thames, Surrey KT1 2EE, UK.

Mineralogical Magazine, April 1997, Vol. 61, pp. 197–212

(e.g. melilite) and it is recognised to be of a primary igneous origin in the melilitolite (Nielsen, 1980, and Nielsen *et al.*, in press). Furthermore, the mineralogy of the melilitolite has been described in detail for most minerals, but only briefly for perovskite and apatite (Nielsen, 1980).

The aims of this work are to describe the composition of perovskite in a variety of selected rock types and to establish the partitioning behaviour of rare earth elements (*REE*) between perovskite and coexisting minerals (apatite, melilite, amphibole, diopside). From this it should be possible to assess the role of perovskite in controlling rare earth and other trace element distributions in the selected rock types.

Analytical methods

Electron probe microanalysis (EPMA)

All mineral compositions were determined by EPMA. The perovskites and apatites were analysed using a Cameca SX50 wavelength dispersive electron probe microanalyser; operating conditions are given in Table 1*a* along with other specifications. Peak overlap determinations were undertaken, and corrections were applied for elements affected by the Ti-*K*α, Ba-*L*α, Ce-*L*α and La-*L*α lines, (Table 1*b*). The silicates were analysed using a Hitachi S2500 SEM equipped with a Link AN10/555 energy dispersive spectrometer, operated at 15 kV and 1 nA specimen current on a V calibration standard.

Instrumental neutron activation analysis (INAA)

Separated grains, ultimately by hand-picking, of perovskite and other minerals were also analysed for most of the *REE* by instrumental neutron activation analysis (INAA). Pure powder or grain samples were first sealed into polyethene ampoules and then irradiated in a 100kW reactor. Appropriate decay periods were allowed before γ-rays were counted twice using an intrinsic Ge detector, and twice using a Ge (Li) detector. The details of the procedures, standards and quality control are described in Williams and Wall (1991). However, it should be mentioned here that although the perovskites are known to contain inclusions of apatites and silicates, small quantities of these low-*REE*-bearing phases would not significantly affect the measured *REE* concentrations of the perovskites.

Results and discussion

Perovskite composition

Major and trace element compositions, determined by EPMA are given in Table 2, together with cation numbers on the basis of 24 oxygen atoms. These data show that perovskite from the rocks of the melilitolite ring dyke (GM 55205 and MM 2553) and the dyke in the pegmatite zone (GM 29977) is perovskite *sensu stricto* (calcium titanate), the only exception being a *REE* variety, loparite, which is from the syenite (GM 29910 B).The analyses compare well with the single published analysis of Gardiner perovskite, by Frisch and Keusen (1977). Small differences of Frisch and Keusen's (1977) analysis of perovskite include lower Nb and *REE* contents (by 1–2 wt.% oxides) than in the present study, and slightly higher Fe and Al.

Many published compositions of perovskites have a small cation excess, e.g. Boctor and Yoder (1982) and Dawson *et al.* (1994). In addition, the Gardiner loparites display a cation excess on the *A* site and a cation deficiency on the *B* site relative to the ideal ABX_3 stoichiometry (Table 2). This phenomenon is tolerated to a certain extent by the perovskite structure, as are small degrees of oxygen excess or deficiency (Mitchell, 1996). Mitchell, (1996), in a detailed discussion of non-stoichiometry, states that perovskites need to be considered as defect structures to explain why many natural compositions plot in the 'forbidden region' of Nickel and McAdam (1963). For the Gardiner compositions, cations have been assigned to *A* and *B* sites as follows, on the basis of charge and ionic radius.

A: Ca, Sr, Y, *REE*, Th, U, Na
B: Ti, Si, Al, Zr, Sn, Nb, Ta, Fe^{3+}

Iron is thought to occupy mainly the *B*-site as ferric Fe. Muir *et al.* (1984) produced Mössbauer spectra of Fe in perovskite from Magnet Cove (USA), and showed that Fe^{3+} was octahedrally co-ordinated. Further evidence is in the perovskite-latrappite coupled substitution; $2Ti^{4+} = Nb^{5+} + Fe^{3+}$, as described below in relation to the present analytical findings. The Gardiner perovskites were also analysed by EPMA for Mg, Mn, K, Cr, Ba, Hf, W and Pb, but none of these elements was detected.

Substitutions. In the perovskites, minor amounts of Na + *REE* (up to about 0.36 atoms of rare earths to 24 oxygens) substitute for Ca, (Fig. 1*a*), and minor amounts of Nb + Fe (up to about 0.09 atoms of Nb to 24 oxygens) substitute for Ti (Fig. 1*b*). The simple, well-known, perovskite-lueshite (Ca + Ti = Na + Nb) substitution of Nickel and McAdam (1963) is shown in Fig. 2 to have an improved correlation for the Gardiner perovskites with the addition of *REE* and Fe to the equation. Hence, the correlation coefficient (r^2) for the combined substitutions, Ca + Ti = (Na + *REE*) + (Nb + Fe), is 0.960. When loparite from the syenite is included, $r^2 = 1.000$ (Fig. 2). Substitution of Sr for Ca is greatest in the loparite, at 0.47 atoms to 24 oxygens, and ranges from approximately 0.05 to 0.13 in the perovskites. Over 1 atom of Nb and over

TABLE 1(b). Peak-overlap correction factors for microprobe analysis of perovskite

Element X-ray line		Interference		Oxide correction factor (%)
Ba	*Lα*	Ti	*Kα*	0.81
Ce	*Lα*	Ti	*Kα*	0.35
Ce	*Lα*	Ba	*Lα*	33.10
Sm	*Lα*	Ce	*Lα*	0.68
Gd	*Lα*	Ce	*Lα*	6.95
Gd	*Lα*	La	*Lα*	1.55

TABLE 1(a). Standards and operating conditions for electron probe microanalysis of perovskite. Beam energy: 20 kV. Beam current: 20 nA

Element X-ray line		Calibration standard	Crystal	Count time (seconds)	Limit of detection (2-σ, oxide wt.%)
Si	*Kα*	Jadeite	TAP	10	0.02
Ti	*Kα*	Ca titanate	PET	10	0.02
Zr	*Lα*	Zircon	PET	10	0.11
Hf	*Lα*	Pure Hf	LIF	20	0.13
Sn	*Lα*	Cassiterite	PET	20	0.03
Th	*Mα*	Pure Th	PET	20	0.09
U	*Mβ*	Pure U	PET	20	0.07
W	*Lα*	Pure W	LIF	20	0.16
Nb	*Lα*	Na niobate	PET	20	0.05
Ta	*Lα*	Pure Ta	LIF	20	0.15
Al	*Kα*	Jadeite	TAP	10	0.04
Cr	*Kα*	Pure Cr	LIF	20	0.04
V	*Lα*	Pure Y	PET	30	0.06
La	*Lα*	La glass *	PET	20	0.04
Ce	*Lα*	Ce glass *	PET	20	0.05
Pr	*Lβ*	Pr glass *	LIF	50	0.09
Nd	*Lα*	Nd glass *	LIF	30	0.10
Sm	*Lα*	Sm glass *	LIF	30	0.06
Gd	*Lα*	Gd glass *	LIF	25	0.13
Fe	*Kα*	Pure Fe	LIF	10	0.07
Mn	*Kα*	Pure Mn	LIF	10	0.08
Mg	*Kα*	Olivine	TAP	20	0.03
Ca	*Kα*	Ca titanate	PET	10	0.03
Sr	*Lα*	Celestine	PET	20	0.05
Ba	*Lα*	Ba fluoride	PET	20	0.05
Pb	*Mα*	Galena	PET	10	0.09
Na	*Kα*	Na niobate	TAP	20	0.02
K	*Kα*	Muscovite	PET	10	0.02
F	*Kα*	Ba fluoride	TAP	20	0.03# (# element %)

*Single-*REE* glasses (Ca, Al silicates) prepared by Peter Hill, (University of Edinburgh).

TABLE 2. Electron microprobe analyses of perovskite-group minerals from the Gardiner Complex

	Perovskite														Loparite	
	MM 2553		GM29919		BM1978,403a		GM 29714		GM 29977				GM 55205		29910B	
Oxide %	Rim	Centre	Rim	Centre	Centre	Rim	Centre	Rim	Centre A	Rim C	Centre B	Rim D	Centre	Rim	Centre	Rim
Nb_2O_5	1.04	0.85		0.83	0.61	0.84	0.79	0.70	0.95		0.83	0.93	0.46		10.51	10.58
Ta_2O_5							0.21								0.59	0.44
SiO_2		0.03		0.04	0.03	0.03			0.06	0.03		0.04	0.04	0.03	0.01	0.04
TiO_2	53.44	54.85	56.56	53.71	53.76	54.69	53.69	55.31	54.72	57.78	53.31	52.82	54.50	57.42	37.29	37.33
ZrO_2		0.15												0.20		
SnO_2	0.05	0.06		0.03	0.06	0.08		0.04			0.04			0.05	0.04	0.05
ThO_2	0.27			0.12								0.09			1.16	1.16
UO_2				0.11	0.08	0.08					0.07				0.08	0.26
Al_2O_3	0.17	0.10	0.13	0.15	0.16	0.16	0.15	0.13	0.23	0.05	0.13	0.27	0.15	0.08		0.07
Fe_2O_3	1.41	1.03	1.17	1.31	1.36	1.10	1.49	1.09	1.50	0.70	2.03	1.87	1.73	1.40	0.17	0.20
Y_2O_3		0.14		0.13	0.12	0.10		0.14	0.08		0.06		0.17		0.07	
La_2O_3	1.29	0.65		0.82	0.86	0.70	1.07	0.71	0.74	0.06	1.03	1.23	0.79		9.38	9.64
Ce_2O_3	2.82	1.11		2.00	1.97	1.44	2.81	1.58	1.29		2.10	2.63	1.82		17.78	18.18
Pr_2O_3	n.d.	n.d.	n.d.	n.d.	n.d.	n.d.	n.d.	n.d.	n.d.	n.d.	n.d.	n.d.	n.d.	n.d.	1.92	1.92
Nd_2O_3	1.03	0.45		0.91	0.88	0.53	1.12	0.68	0.59		0.91	1.04	1.01		5.11	5.00
Sm_2O_3	0.15			0.13	0.17	0.07	0.27	0.10			0.18	0.15	0.26		0.26	0.40
Gd_2O_3				0.18	0.16						0.13				0.62	0.72
CaO	36.09	38.38	40.05	37.27	37.05	38.22	35.71	37.94	38.00	40.29	37.21	36.43	37.57	41.16	2.50	2.53
SrO	0.96	0.71	0.63	0.55	0.74	0.64	0.93	0.58	1.18	0.86	0.62	0.95	0.58	0.46	3.46	2.99
Na_2O	0.89	0.40	0.18	0.54	0.56	0.41	0.75	0.38	0.22	0.24	0.24	0.38	0.52	0.05	9.49	9.27
Total	99.61	98.91	98.72	98.83	98.57	99.09	98.99	99.38	99.56	100.01	98.89	98.83	99.60	100.85	100.44	100.78

(TABLE 2 *contd*)

	Perovskite														Loparite	
	MM 2553		GM29919		BM1978,403a		GM 29714		GM 29977				GM 55205		29910B	
Oxide %	Rim	Centre	Rim	Centre	Centre	Rim	Centre	Rim	Centre A	Rim C	Centre B	Rim D	Centre	Rim	Centre	Rim
Atoms to 24 oxygens																
Nb	0.089	0.072		0.071	0.052	0.071	0.068	0.059	0.080		0.071	0.080	0.039		1.114	1.119
Ta							0.011								0.038	0.028
Si		0.006		0.007	0.006	0.006			0.011	0.006		0.007	0.008	0.005		0.008
Ti	7.621	7.717	7.849	7.650	7.671	7.700	7.682	7.762	7.674	7.915	7.602	7.571	7.677	7.803	6.580	6.570
Zr		0.013												0.018		
Sn	0.004	0.005		0.002	0.005	0.006		0.003			0.003	0.002		0.003	0.003	0.004
Th	0.012			0.005								0.004		0.003	0.062	0.062
U				0.004	0.003	0.003					0.003				0.004	0.014
Al	0.038	0.022	0.029	0.032	0.036	0.035	0.034	0.028	0.049	0.010	0.029	0.062	0.033	0.018		0.018
Fe	0.201	0.145	0.162	0.187	0.195	0.155	0.214	0.153	0.210	0.096	0.290	0.267	0.244	0.190	0.030	0.035
Y		0.014		0.013	0.013	0.010		0.014	0.008		0.006		0.017		0.009	
La	0.090	0.045		0.057	0.060	0.048	0.075	0.049	0.051	0.004	0.072	0.086	0.054		0.812	0.832
Ce	0.196	0.076		0.139	0.137	0.099	0.196	0.108	0.088		0.145	0.183	0.125		1.527	1.558
Pr	n.d.	n.d.	n.d.	n.d.	n.d.	n.d.	n.d.	n.d.	n.d.	n.d.	n.d.	n.d.	n.d.	n.d.	0.164	0.163
Nd	0.070	0.030		0.062	0.060	0.036	0.076	0.045	0.040		0.062	0.071	0.067		0.428	0.418
Sm	0.010			0.008	0.011	0.005	0.018	0.007			0.012	0.010	0.017		0.021	0.032
Gd				0.011	0.010						0.008				0.048	0.056
Ca	7.331	7.692	7.918	7.563	7.531	7.665	7.280	7.585	7.592	7.860	7.558	7.437	7.539	7.966	0.627	0.634
Sr	0.106	0.077	0.067	0.061	0.081	0.070	0.103	0.063	0.128	0.091	0.068	0.104	0.063	0.049	0.471	0.405
Na	0.326	0.143	0.064	0.196	0.204	0.150	0.276	0.136	0.079	0.086	0.088	0.142	0.188	0.018	4.319	4.208
Total A-site	8.141	8.077	8.049	8.119	8.110	8.086	8.024	8.007	7.986	8.041	8.022	8.037	8.070	8.036	8.492	8.382
Total B-site	7.953	7.980	8.040	7.949	7.965	7.973	8.009	8.005	8.024	8.027	7.995	7.989	8.001	8.037	7.765	7.782
Total cations	16.09	16.06	16.09	16.07	16.08	16.06	16.03	16.01	16.01	16.07	16.02	16.03	16.07	16.07	16.26	16.16

n.d. – not determined

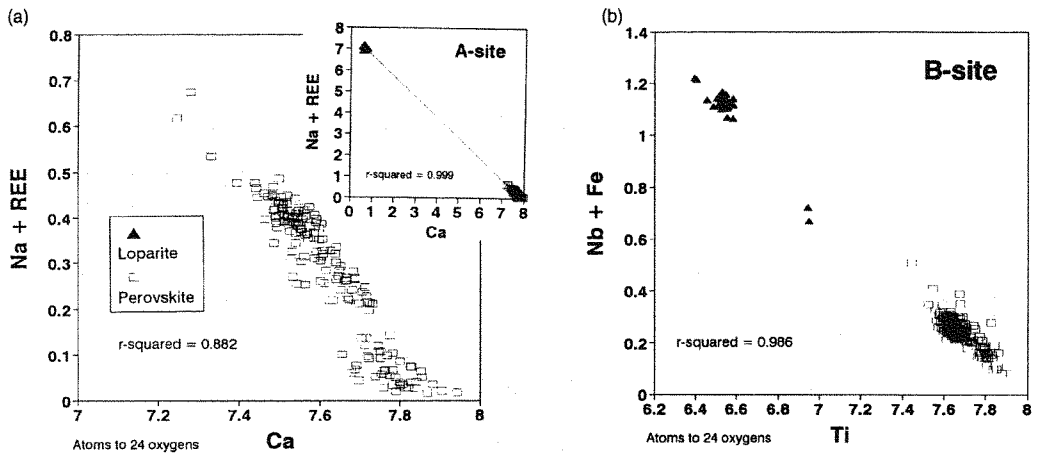

FIG. 1. Minor element substitutions in perovskite and loparite. (*a*) Na + *REE* in the *A*-site; (*b*) Nb + Fe in the *B*-site.

4 atoms of Na, to 24 oxygens, occur in the loparite, but Fe is lower in loparite than in perovskite, at 0.03 atoms to 24 oxygens. Some other trace elements detected include Th and Ta, (up to 0.06 and 0.04 atoms, respectively, in loparite), U, Sn, Si, Al and Zr (Table 2). A positive correlation between Sr and Th (r^2 = 0.667), was revealed for the loparite from specimen GM 29910B (Fig. 3). The concentration of Al, assigned to the *B*-site and negatively correlated with Ti, tends to be higher in perovskite than in loparite and this is probably related to the small size of the Al^{3+} ion.

Trace amounts of F are commonly found in perovskite-group minerals at Gardiner, constituting up to 0.2 wt.% F. However, no relationships between F and any other constituent of perovskite-group minerals of the Gardiner Complex have been identified. The *X* site anion is therefore given as O^{2-}.

Zonation. The complex zonation patterns observed in the perovskites by backscattered electron imaging (supported by EPMA spot-analyses), indicate changes in the crystallization environment during perovskite formation. These patterns have been rationalized into four episodes, best represented by

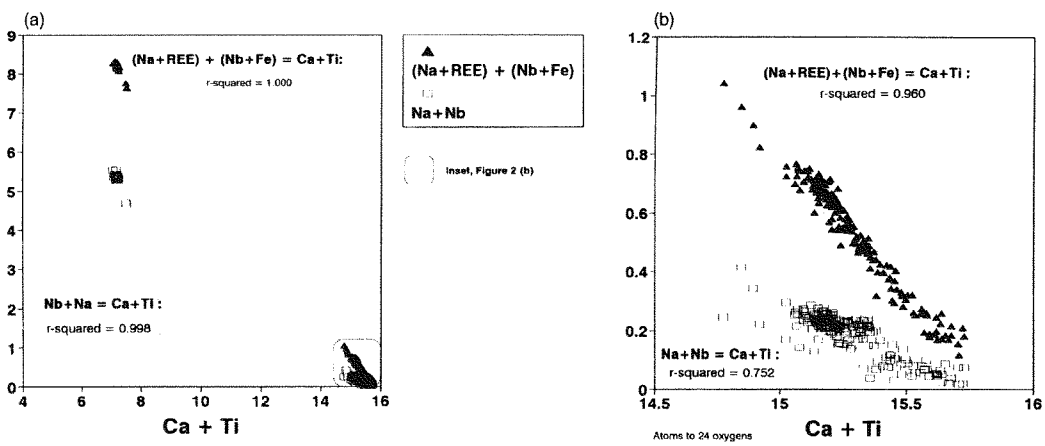

FIG. 2. Minor element substitutions in (*a*) perovskite and loparite and (*b*) perovskite *sensu stricto*. The simple Ca+Ti = Na+Nb type substitution of Nickel and McAdam (1963) is improved with the addition of *REE* and Fe to the equation.

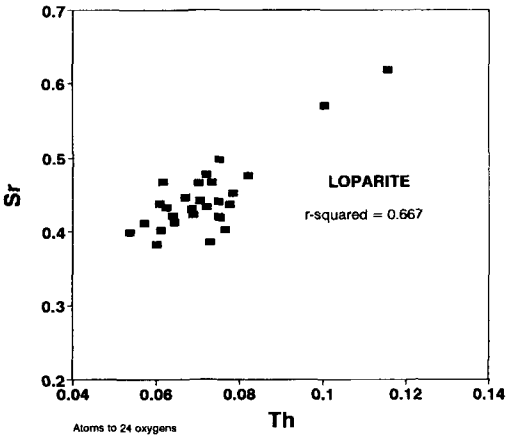

FIG. 3. Correlation of Th and Sr in loparite of rock GM 29910B.

zone types A to D in specimen GM 29977, the dyke rock:

A Central, fairly homogeneous, with ΣREE_2O_3 about 2–4.5 wt.%. Minor, fine scale oscillatory zonation towards rim areas (Figs. 4 and 5).

B Central, homogeneous, blocky, discontinuous zones (Figs. 4*b* and 5). ΣREE_2O_3 over 4 wt.%.

C Rim areas, and mantling magnetite (Figs. 4*b* and 6). Mostly pure $CaTiO_3$ with virtually no detectable trace element substitutions.

D 20–40 μm bands associated with grain boundaries of perovskite (Fig. 6), and containing around 5 wt.% ΣREE_2O_3.

The 'A' core zones are ubiquitous in the specimens studied and the 'C' rim zones are also very common. The *REE*-bearing rim zones (D), of GM 29714 and BM 1978,403a perovskites are very similar in composition to the central, 'A' zones of the other specimens, with over 2.7 wt.% REE_2O_3. Compositional profiles across some grains were undertaken. Figure 4 shows one example where the 'A' core zonation becomes oscillatory toward the 'C' rim adjacent to magnetite. In sample MM 2553, a single, narrow (<5 μm), euhedral growth zone was observed on several large crystals, approximately 300 μm from the rims. This zone was found to be composed of perovskite with over 5 wt.% REE_2O_3, 0.8% Nb_2O_5, 1.1% Fe_2O_3, and 0.6 Na_2O (Fig. 7). The asymmetry of the zone suggests a sudden increase in *REE*, either as a back reaction with *REE*-enriched residua, or from a new influx of fluid. This was immediately followed by a gradual decrease as re-equilibration took place. The irregular, patchy zonation of the rim areas of MM 2553 perovskites indicates further precipitation from *REE*-enriched fluids at a late stage of formation of this rock.

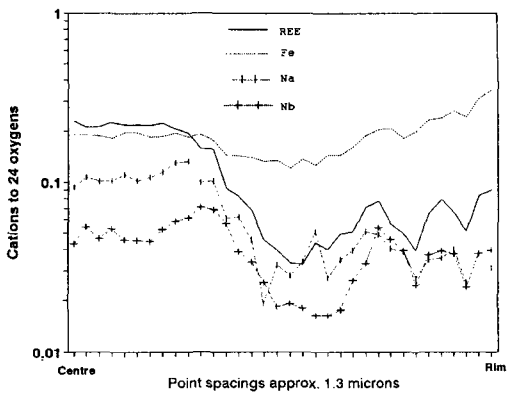

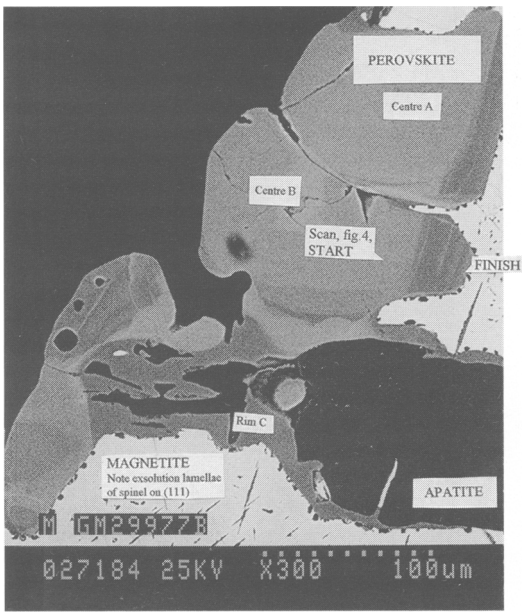

FIG. 4. (*a*) Compositional profile across perovskite from rock GM 29977. The location of the scan is shown in the backscattered-electron image, (b).

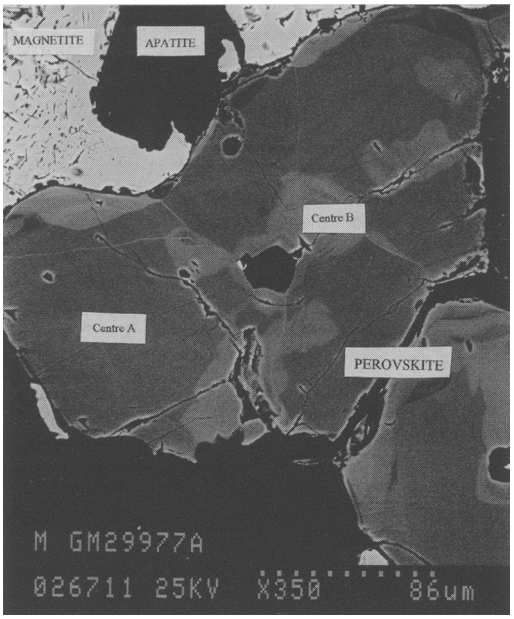

FIG. 5. Homogeneous and blocky central zones (centres A and B respectively) of perovskite in specimen GM 29977.

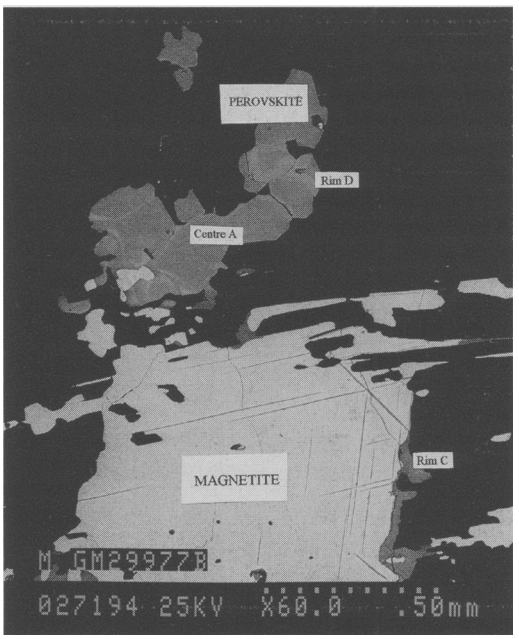

FIG. 6. Perovskite mantling magnetite (rim C), and as separate grains (centre A, with rim D associated with grain boundaries). Magnetite is streaked out along cleavage planes of phlogopite.

Rare earth element chemistry and partitioning

Perovskite. Chondrite-normalized rare earth plots were constructed (Fig. 8*a*–*g*), using both EPMA spot-analysis data (Table 2), and INAA bulk-analysis data (Table 3). Core and rim compositions are represented using the EPMA data, and for specimen GM 29977, the *REE* patterns displayed in three of the four types of zones are shown (Fig. 8*a*). For each specimen there is excellent agreement between the EPMA and the INAA data. As would be expected from the analysis of bulk samples of perovskite, the results from the INAA lie somewhere between the

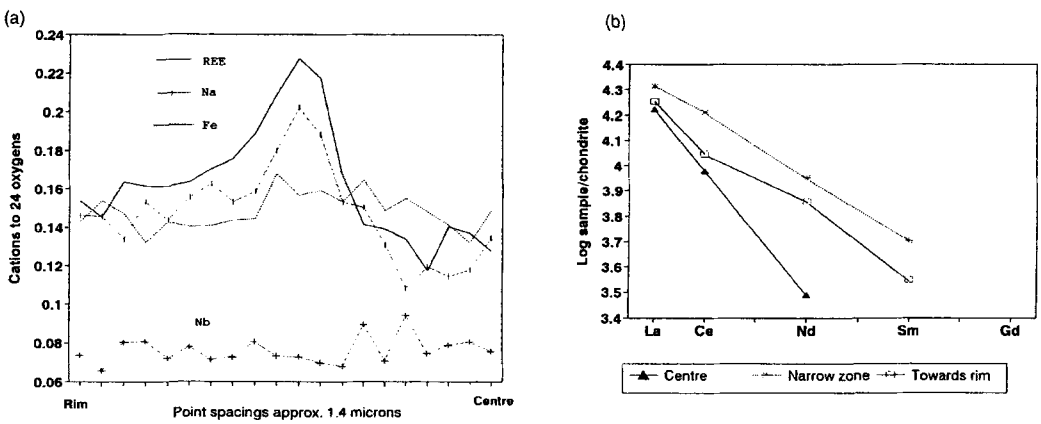

FIG. 7. Narrow growth zone in perovskite of rock MM 2553. (*a*) compositional profile and (*b*) chondrite-normalized rare earth plot of the centre of the grain, the narrow zone, and the rim area.

TABLE 3. Bulk INAA analyses for the *REE* (ppm)

	Perovskite						Apatite				Melilite		Pyroxene		Amphibole
	BM 1978,403a	GM 29714	GM 29977	GM 55205	GM 29919	MM 2553	BM 1978,403a	GM 29714	GM 29977	GM 55205	GM 55205	GM 29919	GM 29977	GM29910B	GM 29910B
La	8000	8900	6920	7660	7200	6340	980	535	1000	780	53	6340	28	26	10
Ce	17290	20150	12260	14180	13250	9410	1220	1062	1390	1070	66	15	53	58	30
Pr															
Nd	6960	7500	5280	6650	7750	3330	530	352	620	520	31	7	31	21	
Sm	1020	1080	890	970	970	660	101	80	126	108	6	1.2	13		
Eu	302	312	232	248	251	210	31	38	41	35	1.9	0.3	2.6	1.4	1.1
Gd	690	670	570	390	620	600	100	116	124	110	7		6		
Tb	82	81	63	64	68	70	10	15	15.3	12.9	0.7		0.9		0.5
Tm	12	17	11	13	11	11	1.2	4.8	3.7		0.1		0.1	0.2	0.4
Yb	19	15	16	45	18	29	8	11	10	8.5	0.3		3.3	4.5	4.9
Lu	0.9	1.1			1.3	2.1		0.7	0.4	0.6			0.4	0.9	

Note: Up to a 30% error can be expected with very low values of Ce, Nd and Tb, as in the melilite, pyroxene and amphibole results.

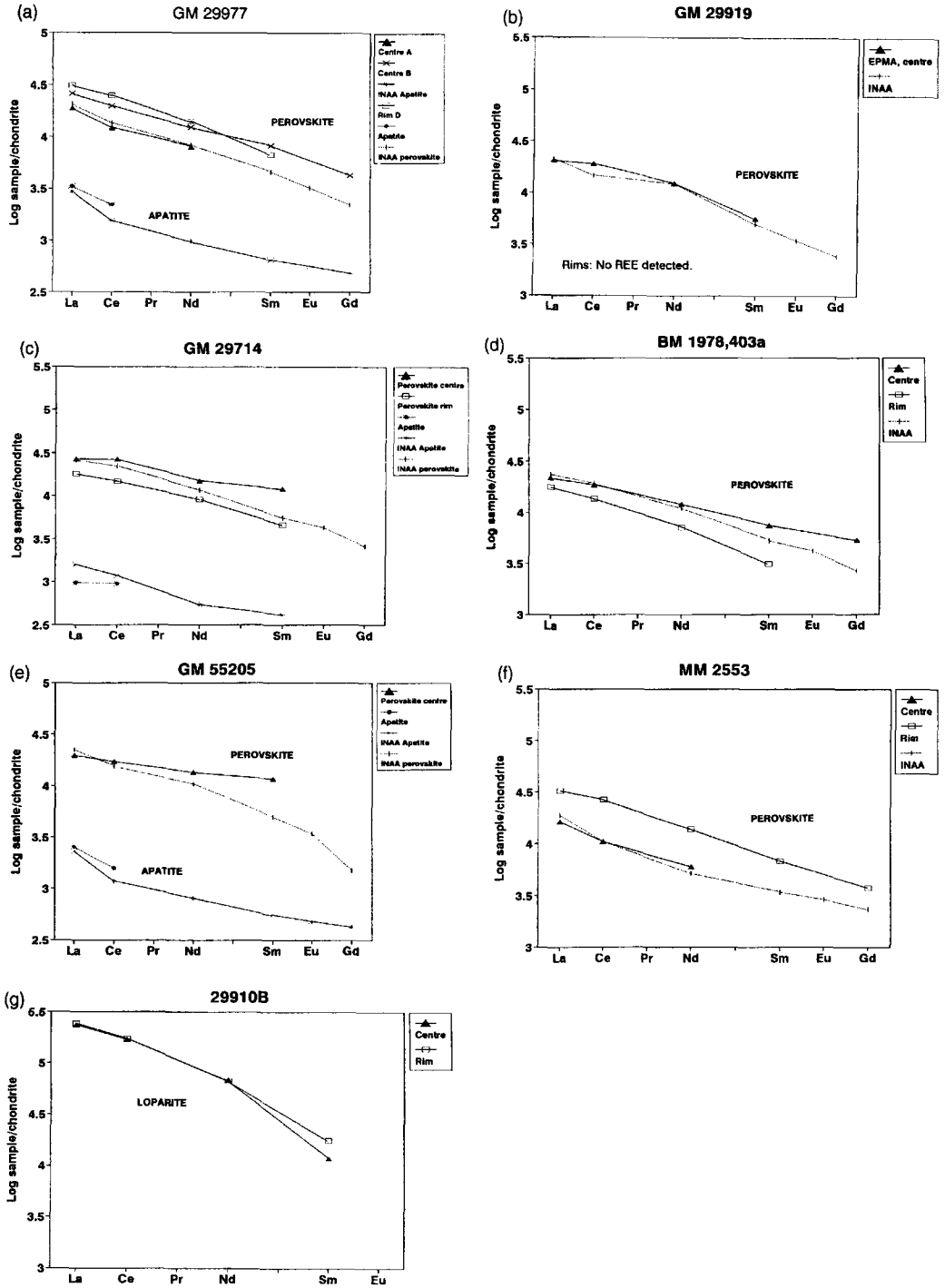

FIG. 8. Chondrite-normalized (Wakita *et al.*, 1971) rare earth plots for perovskite-group minerals and apatite in the seven rocks.

core and rim values obtained by EPMA. This is especially apparent in specimens BM 1978,403a and GM 29714. In the specimens which indicated (from BSE images) that the perovskites were mostly homogeneous with narrow or absent rim zones, the INAA data plot close to the 'core' values (e.g. in GM 29919 and MM 2553, obtained by EPMA). Since a wider range of *REE* (Tb to Lu) are detectable by INAA, the data extending to Lu by this method can be considered representative of the Gardiner perovskite compositions.

Apatite. In Fig. 8*a,c,e* the chondrite-normalized *REE* data for apatite indicate *LREE* enrichment relative to *HREE*, as in the perovskites, and there is good agreement between the INAA data and the partial EPMA results. No zonation was detected in Gardiner apatite.

Rare earth partitioning. The common co-existence of perovskite and apatite in alkaline igneous rocks allows the comparison of rare earth element partitioning in the Gardiner specimens with partitioning recorded for other occurrences and by experiment. The partition coefficient, $K = (M)_{perov.}/(M)_{apatite}$, where M is weight concentration of a trace element in perovskite or apatite, is given for the *REE* in Table 4. The plots in Fig. 9*a–f* show the partitioning of the *REE* between several minerals, perovskite, apatite, melilite, amphibole and diopside. Magnetite was not suitable since it is re-equilibrated, with Ti being expelled from Ti-magnetite. It is likely, also, that Nb, *REE* and other trace elements leave the magnetite. In addition, Gardiner magnetite is always intimately associated with perovskite, and full separation for bulk analysis would not be possible.

Perovskite clearly takes up the *REE* preferentially to the other minerals, as would be expected from previous studies on perovskite and *REE* partitioning, such as in Dawson *et al.* (1994). Most of the phases in the Gardiner samples that were studied display pronounced *LREE* enrichment. Apatite, in turn, has higher concentrations of *REE* than melilite, pyroxene and amphibole. It was not possible (due to quantity of samples available) to determine whole-rock concentrations of *REE* in the specimens. However, it is reported in Wilson *et al.* (1995) that typical melilitites (extrusive equivalents of melilitolites) contain 156 ppm Ce and 1.8 ppm Yb (mean of six rocks from the Upper Rhine graben, Germany) while the perovskites of the Gardiner rocks have up to 2.8 $\times 10^4$ ppm Ce and 108 ppm Yb. Thus perovskites can be a significant contributor to both the abundances and profile of the rare earths in a rock, even when only at minor (about 5%) modal amounts. The perovskites from the Gardiner melilitolites all have similar chondrite-normalized *REE* abundances and patterns, which could suggest an equilibrium distribution. The chemical zonation in perovskite as described earlier is thought to be associated with small, localized fluctuations in magma composition.

The occurrence of loparite in the syenite allows a comparison with the chondrite-normalized *REE* patterns of pyroxene and amphibole in the syenite (Fig. 9*f*). Loparite displays strong *LREE* enrichment, and strong partitioning of *REE* over the silicate phases. According to Veksler and Teptelev (1990) loparite can crystallize directly from natural agpaitic parental magmas. The syenite also contains titanite, indicating that the silica activity and oxygen fugacity of the magma were inappropriate for perovskite (*sensu stricto*) to form (Smith, 1970, and Veksler and Teptelev, 1990). Titanite is also known to accept many trace elements, and it would certainly influence

TABLE 4. Perovskite/apatite partition coefficients, K, for the *REE* in four Gardiner rocks from INAA bulk analyses

	BM1978,403a	GM29714	GM29977	GM55205	Mean K	Standard deviation (n − 1)
La	8.16	16.64	6.92	9.82	10.4	4.3
Ce	14.17	18.97	8.82	13.25	13.8	4.2
Pr						
Nd	13.13	21.31	8.52	12.79	13.9	5.3
Sm	10.10	13.50	7.06	8.98	9.9	2.7
Eu	9.87	8.21	5.66	7.09	7.7	1.8
Gd	6.90	5.78	4.60	3.55	5.2	1.5
Tb	7.88	5.44	4.12	4.96	5.6	1.6
Tm	10.00	3.54	2.97		5.5	3.9
Yb	2.50	1.33	1.60	5.29	2.7	1.8
Lu		1.57			1.6	

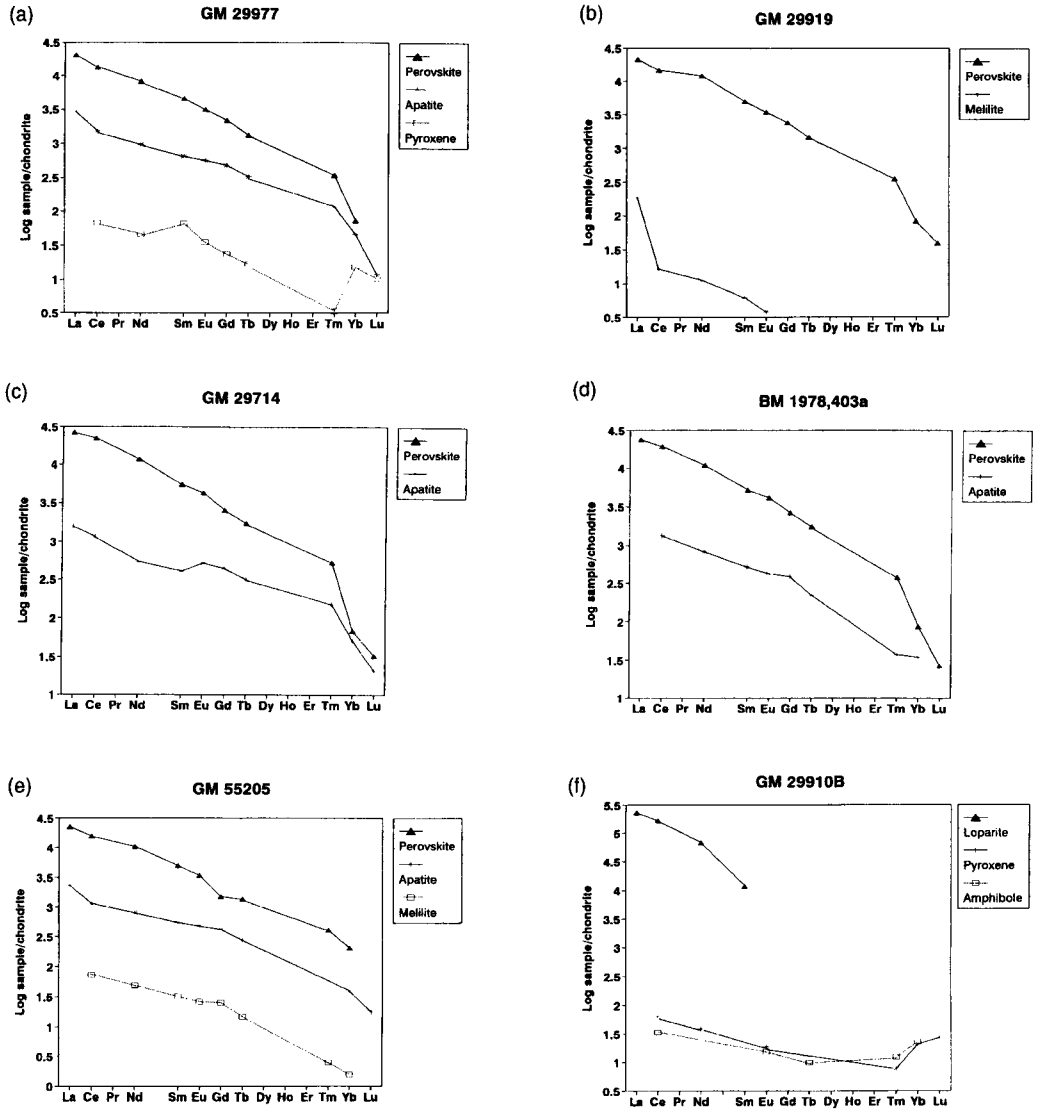

FIG. 9. Chondrite-normalized rare earth plots for perovskite, apatite, melilite and pyroxene, and for loparite, pyroxene and amphibole.

the partitioning behaviour of the *REE* in the presence of perovskite (Dawson *et al.*, 1994), but no data for Gardiner titanites are available.

Rare earth partition coefficients for apatite-silicate melt systems have been determined by several authors (e.g. Nagasawa, 1970; Nagasawa and Schnetzler, 1971; Watson and Green, 1981; and Wörner *et al.*, 1983). The values recorded by Nagasawa (1970) for an apatite–dacite system are similar to those reported by Wörner *et al.* (1983) for an apatite–phonolite system. However, the data of Wörner *et al.* (1983) show greater fractionation between middle members of the *REE* (such as Sm and Tb) and both light and heavy *REE*.

In order to obtain an approximate value for the *REE* partition between Gardiner perovskite and melt we have averaged the four INAA data sets from Table 4 for perovskite/apatite partition and then related this average to the experimental data of Watson and Green (1981), for apatite/liquid partition in their basanite-

811. The calculated perovskite/liquid partition coefficients for Gardiner are given in Table 5 and are similar to those of Onuma *et al.* (1981) for perovskite in a melilite-nepheline basaltic melt. However, the data differ significantly from those of Simon *et al.* (1994) on experimental Ca,Al-rich compositions.

Using the Onuma *et al.* (1981) data we may establish the approximate nature of the chondrite-normalized *REE* pattern in the Gardiner magma. Based on the GM 29714 perovskite analyses, the pattern for the magma shows significant relative enrichment in the light rare earths, with a chondrite-normalized La/Lu of 235, La/Sm of 6.2 and Sm/Lu of 41. However, fractional crystallisation of only a small volume of perovskite causes a significant change in the liquid composition. For example, crystallisation of 2.5% of perovskite alone would change the chondrite-normalized La/Lu ratio to about 165, and reduce the La concentration to about 0.6 of its previous value. Thus, perovskite can play a determining role in magma composition during fractional crystallisation processes, even when at the abundance levels found in the Gardiner intrusion.

Conclusions

The excellent agreement between the INAA and the EPMA results for the *REE* demonstrates that the full range of *REE* as well as their zoned distribution, can be readily investigated. Using the calculated mineral/mineral partition coefficients and data from other published studies, some of the L*REE* enrichment in perovskite can be attributed to a crystal chemical control, but with enrichment occurring in all the phases studied, magmatic fractionation is also indicated. Perovskite has provided a sink for a multitude of other trace elements, reaffirming the known ability of the perovskite structure to be able to accept a wide range of trace elements.

Acknowledgements

C.T. Williams is thanked for his assistance in the analytical work, and O. Johnsen is thanked for specimen GM 29714. The manuscript has benefitted from helpful suggestions by two reviewers.

References

Boctor, N.Z. and Yoder Jr., H.S. (1982) Distribution of rare earth elements in perovskite from melilite-bearing rocks. *Yearbook of the Carnegie Institution, Washington*, **81**, 369–71.

Dawson, J.B. (1994) Quaternary kimberlitic volcanism on the Tanzania Craton. *Contrib. Mineral. Petrol.*, **116**, 473–85.

Dawson, J.B., Smith, J.V. and Steele, I.M. (1994) Trace-element distribution between coexisting perovskite,

TABLE 5. Perovskite/liquid partition coefficients for the *REE*

	Gardiner (Calculated from apa/liq of basanite 811 of *Watson and Green, 1981, and per/apa of this study #, Table 3.)	Other examples		
	Perovskite/liquid : (apa/liq)* × (per/apa)#	Onuma *et al.*, (1981) Perovskite/groundmass : melilite-nepheline basalt	Dawson, (1994) Perovskite/bulk lava : kimberlitic lava	Simon *et al.*, (1994) Perovskite/liquid : experiment QPX-8
La	27	20.3	55.8	4.7
Ce		22.2	74.5	
Pr			83.9	
N		25	85.8	
Sm	46.5	26.8	76.1	5.2
Eu		23	59.6	
Gd			46.6	
Tb				
Dy	4.2	14	46.7	
Ho			22.1	
Er			37.6	
Tm				
Yb			15.9	0.51
Lu		5.9	5.0	

* Apa/liq (Watson and Green, 1981): La 2.6, Sm 4.7, Dy 4.2, Lu 1.8.

apatite and titanite from Oldoinyo Lengai, Tanzania. *Chem. Geol.*, **117**, 285–90.

Frisch W. and Keusen H. (1977) The Gardiner Intrusion, an ultramafic complex at Kangerdlugssuaq, east Greenland. *Grønlands Geologiske Undersøgelse Bulletin*, **122**, 62.

Gleadow, A.J.W. and Brooks, C.K. (1979) Fission track dating, thermal histories and tectonics of igneous intrusions in East Greenland. *Contrib. Mineral. Petrol.*, **71**, 45–60.

Johnsen, O., Petersen, O. V. and Medenbach, O. (1985) The Gardiner Complex, a new locality in Greenland. *Mineral. Record*, **16**, 485–94.

Mitchell, R.H. (1996) Perovskites: A revised classification scheme for an important rare earth element host in alkaline rocks. In *Rare Earth Minerals. Chemistry, Origin and Ore Deposits* (A.P. Jones, F. Wall and C.T.W. Williams, Eds.) Mineralogical Society Series, **7**, 41–76. Chapman and Hall.

Muir I.J., Metson J.B. and Bancroft G.M. (1984) (57)Fe Mössbauer spectra of perovskite and titanite. *Canad. Mineral.*, **22**, 689–94.

Nagasawa, H. (1970) Rare earth concentrations in zircons and apatites and their host dacites and granites. *Earth Planet. Sci. Lett.*, **9**, 359–64.

Nagasawa, H. and Schnetzler, C.C. (1971) Partitioning of rare earth, alkali and alkaline earth elements between phenocrysts and acidic igneous magma. *Geochim. Cosmochim. Acta*, **35**, 953–68.

Nickel, E.H. and McAdam, R.C. (1963) Niobian perovskite from Oka, Quebec; A new classification for minerals of the perovskite group. *Canad. Mineral.*, **7**, 683–97.

Nielsen T.F.D. (1979) The occurrence and formation of Ti-aegirines in peralkaline syenites. An example from the Tertiary ultramafic alkaline Gardiner complex, East Greenland. *Contrib. Mineral. Petrol.*, **69**, 235–44.

Nielsen, T.F.D. (1980) The petrology of a melilitolite, melteigite, carbonatite and syenite ring dike system, in the Gardiner complex, East Greenland. *Lithos*, **13**, 181–97.

Nielsen, T.F.D. (1981) The ultramafic cumulate series, Gardiner Complex, East Greenland; cumulates in a shallow level magma chamber of a nephelinitic volcano. *Contrib. Mineral. Petrol.*, **76**, 60–72.

Nielsen, T.F.D. (1994) Alkaline dyke swarms of the Gardiner Complex and the origin of ultramafic alkaline complexes. *Geochemistry International*, **31**, 37–56.

Nielsen, T.F.D. and Holm P.M. (1993) Nd and Sr isotope compositions from the Gardiner Complex, East Greenland Tertiary igneous province. *Bull. Geol. Soc. Denmark*, **40**, 280–7.

Nielsen, T.F.D., Solovova, I.P. and Veksler, I.V. (in press) Parental melts for plutonic melilitolites and alkaline carbonatites: Evidence from crystalline melt inclusions in melilitolites from the Gardiner complex, East Greenland. *Contrib. Mineral. Petrol.*

Onuma, N., Ninomiya, S. and Nagasawa, H. (1981) Mineral/groundmass partition coefficients for nepheline, melilite, clinopyroxene and perovskite in melilite-nepheline basalt, Nyiragongo, Zaire. *Geochem. J.*, **15**, 221–8.

Simon, S.B., Kuehner, S.M., Davis, A.M., Grossman, L., Johnson, M.L., and Burnett, D.S. (1994) Experimental studies of trace element partitioning in Ca,Al-rich compositions: Anorthite and perovskite. *Geochim. Cosmochim. Acta*, **58**, 1507–23.

Smith, A.L. (1970) Sphene, perovskite and coexisting Fe-Ti oxide minerals. *Amer. Mineral.*, **55**, 264–9.

Veksler, I.V. and Teptelev, M.P. (1990) Conditions for crystallization and concentration of perovskite-type minerals in alkaline magmas. *Lithos*, **26**, 177–89.

Wakita, H., Rey, P. and Schmitt, R.A. (1971) Abundances of the 14 rare-earth elements and 12 other trace elements in Apollo 12 samples: five igneous and one breccia rocks and four soils. *Proc. Second Lunar Sci. Conf.*, **2**, The M.I.T. Press, 1319–29.

Watson, E.B. and Green, T.H. (1981) Apatite/liquid partition coefficients for the rare earth elements and strontium. *Earth Planet. Sci. Lett.*, **56**, 405–21.

Williams, C.T. and Wall, F. (1991) An INAA scheme for the routine determination of 27 elements in geological and archaeological samples. *British Museum Occasional Papers: Neutron Activation and Plasma Emission Spectrometric Analysis in Archaeology, Techniques and Applications*. **82**, 105–19.

Wilson, M., Rosenbaum, J.M. and Dunworth, E.A. (1995) Melilitites: partial melts of the thermal boundary layer? *Contrib. Mineral. Petrol.*, **119**, 181–96.

Wörner, G., Beusen, J.-M., Duchateau, N., Gijbels, R. and Schmincke, H.-U. (1983) Trace element abundances and mineral/melt distribution coefficients in phonolites from the Laacher See Volcano (Germany). *Contrib. Mineral. Petrol.*, **84**, 152–73.

[*Manuscript received 28 March 1996: revised 29 August 1996*]

Appendix: Rock descriptions and mineral assemblages

GM 55205 Layered melilitolite.

Medium to coarse grained, layered on scale of 2-10 mm, contains melilite (~60%), magnetite (~20%), perovskite (~10%), phlogopite (~6%) and apatite (~4%). Additionally, minor diopside, Mg-hastingsite, and monticellite. Subhedral perovskite, with minimal, diffuse zonation is closely associated with anhedral magnetite, frequently mantling magnetite grains. Perovskite forms discontinuous layers alternating with melilite-rich areas, and often contains inclusions. Anhedral, inclusion-free apatite, and large phlogopite grains ($\leq$1 cm), are concentrated in perovskite-magnetite layers.

Melilite
$(Ca_{0.85}Na_{0.15})_2(Mg_{0.21}Fe_{0.02}Al_{0.11}Si_{0.66})_3O_7$

Phlogopite
$(Na_{0.31}K_{0.65}Ca_{0.01}Ba_{0.03})_2(Mg_{0.8}Fe_{0.06}Ti_{0.01}Al_{0.13})_6(Si_{0.76}Al_{0.24})_8O_{20}(OH,F)_4$

Diopside
$Ca(Mg_{0.91}Fe_{0.07}Ti_{0.02})(Si_{0.97}Al_{0.03})_2O_6$

Mg-hastingsite
$(Na_{0.93}K_{0.07})Ca_2(Mg_{0.76}Fe_{0.12}Al_{0.11}Ti_{0.01})_5(Si_{0.82}Al_{0.18})_8O_{22}(OH)_2$

Monticellite
$Ca(Mg_{0.78}Fe_{0.21}Mn_{0.01})SiO_4$

MM 2553 Coarse-grained perovskitite within melilitolite

Perovskite (~95%) cumulate within melilitolite. Zoned, sub- to euhedral crystals up to 1 cm, with interstitial nepheline(?), vesuvianite(?), calcite and 50 μm titanite rosettes concentrated on perovskite surfaces. Perovskite is concentrically zoned; central inclusions of acicular apatite, surrounded by a zone rich in inclusions of titanite, pectolite, baryte, strontianite and Fe-Ti oxides, and a rim area relatively inclusion-free. Fine-scale (1–2 μm), discontinuous compositional zonation mostly restricted to fragmented rims and fractures. A single, 5 μm zone marks an earlier, euhedral growth close to rims, and is crosscut by the fine scale zonation.

GM 29919 Melilitolite rock

Melilite (~50%), perovskite (~25%), magnetite (~10–15%), and Mg-hastingsite, ($\leq$10%). Monticellite, widespread but minor (<1%), and ubiquitously associated with fragmented melilite rims. Unzoned, prismatic melilites ($\leq$2 mm wide), display a preferred alignment alternating with, and parallel to, string-clusters of perovskite-magnetite, forming a discontinuous layered fabric on a scale of 0.5–3 mm. Anhedral, secondary Mg-hastingsite ($\leq$1 mm), is patchy and restricted to edges of melilites and perovskite-magnetite clusters. Perovskite, as subhedral, rounded octahedra, occurs both in string clusters alternating with, and as discrete grains within, melilite. Rounded, multiphase inclusions, considered to be crystalline melt inclusions, are described by Nielsen *et al.*, (in press) and occupy central regions of perovskites. Some of the phases in these melt inclusions do not occur in the main rock. Irregular zonation is minimal in perovskite rims. Pure $CaTiO_3$ as the late product of ilmenite/ulvöspinel reaction, mantles magnetite as well as earlier perovskite.

Melilite
$(Ca_{0.85}Na_{0.15})_2(Mg_{0.21}Fe_{0.03}Al_{0.1}Si_{0.66})_3O_7$

Diopside*
$(Ca_{0.92}Sr_{0.03}Na_{0.05})(Mg_{0.8}Fe_{0.19}Ti_{0.01})(Si_{0.98}Al_{0.02})_2O_6$

Mg-hastingsite
$(Na_{0.87}K_{0.13})(Ca_{0.95}Sr_{0.05})_2(Mg_{0.74}Fe_{0.16}Al_{0.08}Ti_{0.02})_5(Si_{0.79}Al_{0.21})_8O_{22}(OH)_2$

Monticellite
$Ca(Mg_{0.73}Fe_{0.25}Mn_{0.01})SiO_4$

Nepheline*
$Na_6(Na_{0.96}Ca_{0.04})_2(Si_{0.49}Al_{0.51})_{16}O_{32}$

* From crystalline melt inclusions in perovskite.

GM 29977. Dyke rock, glimmerite

Medium grained dyke rock containing phlogopite (~40–50%), fluorapatite (~15–20%), and magnetite (~10–15%) clustered with perovskite (~5%). Minor interstitial diopside encloses traces of Ti-andradite. Mg-hastingsite, mostly in rim perovskite as prismatic grains (~100 μm), occasionally crosscuts magnetite-perovskite boundaries. Perovskite is zoned. Magnetite as anhedral masses ($\leq$1 mm), with rim areas streaked out along cleavage planes of phlogopite or interstices of perovskite clusters. Rare inclusions, (perovskite and apatite), but common exsolution lamellae of spinel ($\leq$10 μm) along (111). Apatite as large ($\leq$1 cm), euhedral, prismatic grains, and rarely as inclusions in perovskite, magnetite and diopside. Abundant tubular fluid inclusions in most apatites.

Phlogopite
$(Na_{0.1}K_{0.84}Ba_{0.06})_2(Mg_{0.72}Fe_{0.12}Ti_{0.06}Al_{0.1})_6(Si_{0.72}Al_{0.28})_8O_{20}(OH,F)_4$

Diopside
$(Ca_{0.97}Sr_{0.03})(Mg_{0.68}Fe_{0.25}Ti_{0.07})(Si_{0.82}Al_{0.18})_2O_6$

Mg-hastingsite
$(Na_{0.83}K_{0.17})(Ca_{0.95}Sr_{0.05})_2(Mg_{0.65}Fe_{0.22}Al_{0.08}Ti_{0.05})_5(Si_{0.75}Al_{0.25})_8O_{22}(OH)_2$

Andradite
$(Ca_{0.99}Mg_{0.01})(Al_{0.4}Fe_{0.44}Ti_{0.16})_2(Si_{0.95}Al_{0.05})_2O_{12}$

GM 29910B Loparite-bearing syenite.

Coarse-grained syenite with altered, subhedral perthitic phenocrysts, $\leq$1 cm, (~50%), aegirine (~20%), and

highly altered K-feldspar groundmass, <2 mm (~25%), with minor loparite, ancylite, Sr-celsian, davyne(?), delindeite(?), titanite, rutile, and lorenzenite with vinogradovite overgrowths. Subhedral, pseudocubic loparites (~0.5 mm), are unzoned, and contain inclusions of K-feldspar and aegirine. Aegirine, usually euhedral, occurs as elongated, prismatic phenocrysts (≤2 × 10 mm), in random orientation.

Aegirine

$(Na_{0.87}Ca_{0.13})(Fe_{0.70}Mg_{0.16}Ti_{0.11}Al_{0.03})Si_2O_6$

GM 29714 (Lens in layered melilitolite) and BM 1978,403a

Coarse-grained perovskite (~50%), apatite (~45%) and phlogopite (~4%). BM 1978,403a additionally contains minor diopside. In both rocks perovskite occurs as euhedral, pseudo-octahedra (≤1 cm), with apatite (≤2 mm), and phlogopite (≤1 mm). No layering was detectable in the specimens studied (specimen size; <3 cm^3). Large, (~0.3 mm) inclusions of apatite occur in perovskite in both specimens.